

# Multimodal Representation Learning Conditioned on Semantic Relations

Yang Qiao<sup>1</sup>, Yuntong Hu<sup>1</sup>, Liang Zhao<sup>1</sup>

<sup>1</sup>Emory University

yang.qiao@emory.edu, yuntong.hu@emory.edu, liang.zhao@emory.edu

## Abstract

Multimodal representation learning has advanced rapidly with contrastive models such as CLIP, which align image-text pairs in a shared embedding space. However, these models face limitations: (1) they typically focus on image-text pairs, underutilizing the semantic relations across different pairs. (2) they directly match global embeddings without contextualization, overlooking the need for semantic alignment along specific subspaces or relational dimensions. To address these issues, we propose Relation-Conditioned Multimodal Learning (RCML), a framework that learns multimodal representations under natural-language relation descriptions to guide both feature extraction and alignment. Our approach constructs many-to-many training pairs linked by semantic relations and introduces a relation-guided cross-attention mechanism that modulates multimodal representations under each relation context. The training objective combines inter-modal and intra-modal contrastive losses, encouraging consistency across both modalities and semantically related samples. Experiments on different datasets show that RCML consistently outperforms strong baselines on both retrieval and classification tasks, highlighting the effectiveness of leveraging semantic relations to guide multimodal representation learning.

## 1 Introduction

Multimodal data is increasingly prevalent across domains such as e-commerce, social media, and scientific publishing. Learning unified representations from such data is crucial for enabling understanding, comparison, and generalization across modalities. Due to the lack of large-scale labeled data, contrastive learning has become the dominant approach for this goal (Arora, Liang, and Ma 2019; Names 2024), as it learns from weakly paired samples by aligning matched imagetext pairs while separating mismatched ones. This paradigm was pioneered by CLIP (Radford et al. 2021), which has since inspired rapid progress along several directions: data-centric scaling, label-supervised extensions, augmentation-enhanced variants, loss reformulations, and modality expansion.

Despite their success, these methods share several key limitations. First, they typically focus on image-text pairs, underutilizing the rich web of semantic relations that naturally exist across samples (e.g., different products, papers,

etc.). Second, they match global embeddings directly without contextualization, failing to capture alignment along specific semantic dimensions such as function or style. These challenges are not merely technical, but have tangible impact in real-world use cases. For example, in baby product recommendation, a user focused on infant feeding may consider nursing pillows, milk storage bags, and bottle sterilizers to be closely related. These items span different categories and vary in both appearance and textual description, yet become meaningfully connected under the shared context of infant feeding. Similar issues arise in scientific literature, where content from different papers becomes related under a common methodological theme. On social media, posts about saving money or holiday planning may appear diverse in form but are connected by shared intent. These examples highlight the need to move beyond isolated pairwise contrast, toward modeling sample-level relations within and across modalities to support more contextual and semantically grounded representation learning. Existing works on graphs primarily focus on graph-level embedding, rather than the encoding of images and texts under semantic relations, which is the focus of this paper.

To address these limitations, we propose the Relation-Conditioned Multimodal Learning (RCML) framework, which integrates semantic relations between samples into the representation learning process. Instead of relying on isolated imagetext pairs, RCML constructs training pairs based on natural-language relations, allowing the model to learn from broader inter-sample structures. It further introduces a relation-guided cross-attention contrastive structure, where relation semantics act as conditioning signals to guide feature interaction and alignment across modalities under specific relational contexts. Finally, RCML includes a contrastive objective that jointly captures cross-modal alignment and intra-modal consistency among related samples. Together, these designs enable RCML to learn contextually grounded and relation-aware representations. Our contributions are summarized as follows: (1) We propose RCML framework that uses semantic relations to guide contextual feature extraction, allowing the model to encode modality-specific information under relational perspectives. (2) We enable contrastive learning across semantically diverse samples by modeling many-to-many inter-sample relations, going beyond traditional pairwise alignment or label-

supervised grouping. (3) We conduct comprehensive experiments across seven domains, showing that our method consistently outperforms strong baselines on retrieval and classification tasks.

## 2 Related Work

### 2.1 Multimodal Representation Learning

Many recent models aim to learn unified representations from multiple modalities such as images and text. Models such as CLIP (Radford et al. 2021) and ALIGN (Jia et al. 2021) train on large-scale web-curated imagetext pairs, while later efforts such as LAION (Schuhmann et al. 2022) and DataComp (Gadre et al. 2023) focus on scaling and curating training data at web scale. Subsequent works have explored various ways to improve learning: UniCL and LiT (Yang et al. 2022; Zhai et al. 2022) incorporate label supervision to relax strict pairwise alignment, but ultimately still rely on grouping samples under the same class; DeCLIP and SLIP (Li et al. 2021; Mu et al. 2021) use data augmentation and auxiliary objectives to enforce consistency across different views of the same sample, but do not model relations across distinct samples; SigLIP (Touvron et al. 2023) reformulates the contrastive loss using a sigmoid-based objective, and ImageBind (Girdhar et al. 2023) extends joint representation learning to six modalities. Despite their success, these methods generally overlook the semantic relations that exist across different samples. In particular, they lack mechanisms to guide feature extraction under relational context or to align representations across and within modalities based on inter&intra-sample semantics.

### 2.2 Graph-Based Multimodal Learning

Graph-based approaches have been widely used to model structural relationships in multimodal data. Some methods construct graphs over image and text entities and apply graph neural networks (Kipf and Welling 2017; Veličković et al. 2018) to learn node or graph-level representations (Yao et al. 2019; Jiang et al. 2020; Chen et al. 2020; Qiao et al. 2023; Liu et al. 2020; Wang et al. 2022a). More recently, M2GCN (Zhang et al. 2023) proposes a multimodal graph network that learns sample-level representations in a unified graph structure. While these works explicitly construct and learn over graph structures, our method focuses solely on encoding image and text features. Semantic relations are not used to define a graph, but rather serve as contextual signals that guide the feature extraction process.

### 2.3 Context-Conditioned Multimodal Learning

Recent models such as Flamingo (Alayrac et al. 2022), GIT (Wang et al. 2022b), and BLIP-2 (Li et al. 2023) condition feature extraction on task-specific prompts, typically designed for downstream tasks like captioning or QA. In contrast, our method uses semantic relations between samples as intrinsic conditioning signals for feature encoding.

## 3 Methodology

In this section, we first introduce the overall formulation of relation-conditioned contrastive learning, and then describe

two key components that support it: relation-guided pair construction and contextual feature modulation.

### 3.1 Relation-Conditioned Contrastive Learning

As shown in Figure 1, each sample is denoted as  $V_i = (T_i, I_i)$ , where  $T_i$  and  $I_i$  are the textual and visual descriptions of the item. Pairs of samples  $(V_i, V_j)$  are associated with a natural-language semantic relation  $e_{ij}$ , which serves as contextual guidance for representation learning. When  $i \neq j$ ,  $e_{ij}$  encodes inter-sample semantic relation, illustrated by the yellow or red connections in Figure 1. When  $i = j$ ,  $e_{ii}$  reflects intra-sample semantic relation, depicted as blue connections in the figure (see Section 3.2 for details). Our goal is to learn an encoder  $\mathcal{F}_\theta$  that produces relation-conditioned features  $\mathbf{z}_T(e_{ij})$  and  $\mathbf{z}_I(e_{ij})$  for each sample under the contextual semantics relation of  $e_{ij}$ .

Unlike traditional contrastive learning that operates only on matched pairs (i.e., the diagonal of the similarity matrix), our approach supports many-to-many alignment across samples linked by semantic relations. This is visualized in the colored regions of the similarity matrices in Figure 1, where multiple off-diagonal entries are treated as positive pairs, each conditioned on a distinct relation. Different colors correspond to different semantic contexts, indicating that we extract features specifically modulated by the meaning of each  $e_{ij}$  rather than relying on a single global embedding.

To optimize such relation-aware alignment, we define a contrastive objective that operates over contextualized features. Beyond cross-modal alignment, we incorporate intra-modal consistency by enforcing that text and image features are coherent under the same semantic relation. Specifically, we design a unified loss with three components: (1) text-to-image and image-to-text contrast for cross-modal consistency, and (2) text-text and (3) image-image contrast for intra-modal coherence. This formulation enables RCML to learn features that are semantically aligned both across and within modalities, all under the conditioning of relation descriptions. The overall loss is given by:

$$\mathcal{L} = (\mathcal{L}_{\text{txt-img}} + \mathcal{L}_{\text{img-txt}}) / 2 + \lambda (\mathcal{L}_{\text{txt-txt}} + \mathcal{L}_{\text{img-img}}), \quad (1)$$

where each term follows the same contrastive formulation:

$$\mathcal{L}_{x-y} = - \sum_{(i,j) \in \mathcal{P}} \log \frac{\exp(\text{sim}(\mathbf{z}_x^i(e_{ij}), \mathbf{z}_y^j(e_{ij}))/\tau)}{\sum_{k \in \mathcal{N}(i)} \exp(\text{sim}(\mathbf{z}_x^i(e_{ij}), \mathbf{z}_y^k(e_{ij}))/\tau)}, \quad (2)$$

where  $x, y \in \{\text{txt}, \text{img}\}$  and  $\tau$  is a temperature parameter. Relation-conditioned features  $\mathbf{z}_x^i(e_{ij})$  is defined in Section 3.3, and the construction of positive/negative samples is described in Section 3.2.

### 3.2 Relation-Conditioned Pair Construction

A key component of contrastive learning is the construction of positive and negative sample pairs. In our framework, the positive set  $\mathcal{P}$  consists of all sample pairs  $(V_i, V_j)$  that are explicitly associated with a semantic relation  $e_{ij}$ . These relations are provided as natural-language descriptions and later used to condition feature extraction (Section 3.3). We categorize such positive pairs into two types:

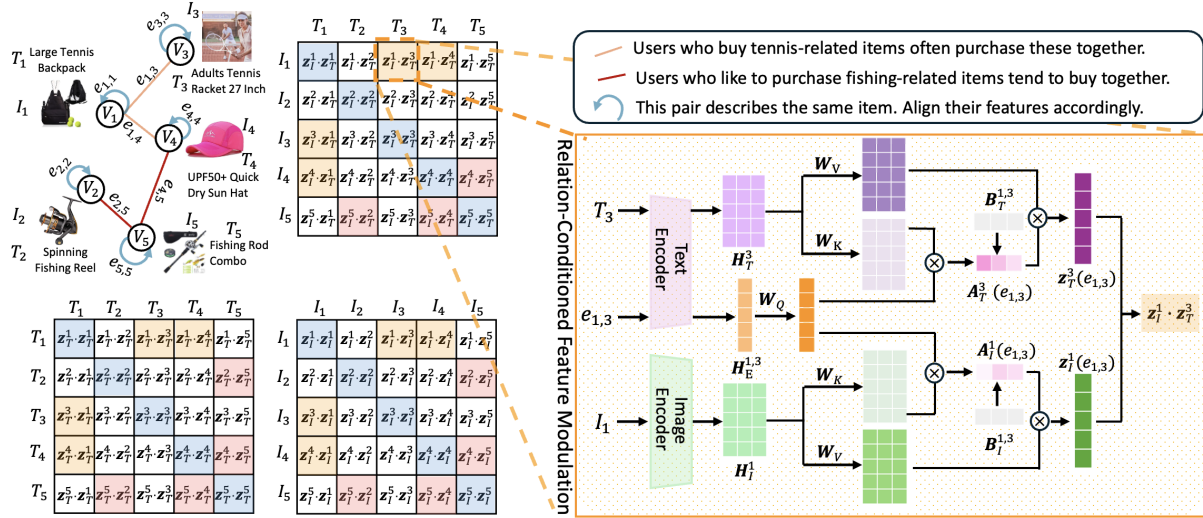


Figure 1: **Overview of the proposed framework.** Each sample consists of a text image pair. Colored elements (red, yellow, blue) represent different semantic relations, which are consistently reflected in sample connections, similarity matrix entries, and feature extraction paths.

**Intra-sample Relations.** These involve the text and image of the same sample  $V_i = (T_i, I_i)$ , paired under a generic semantic relation that indicates both views describe the same item. This encourages the model to align textual and visual modalities within a single sample.

**Inter-sample Relations.** These link different samples  $(V_i, V_j)$  through descriptions that capture semantic associations such as co-purchase, stylistic similarity, or functional complementarity. The relation text  $e_{ij}$  serves as contextual input to guide relation-aware feature extraction.

The negative set  $\mathcal{N}(i)$  for a given anchor sample  $V_i$  consists of unrelated samples randomly drawn from the batch that are not paired with  $V_i$  under any semantic relation. Each positive pair  $(i, j) \in \mathcal{P}$  is contrasted against these negatives using the relation description  $e_{ij}$ , as defined in Equation (2).

### 3.3 Relation-Conditioned Feature Modulation

We utilize CLIP to encode multimodal information for both nodes and edges. Given a sample  $V_i \in \mathcal{V}$ , its textual tokens  $T_i$  and image patches  $I_i$  are passed through the CLIP text encoder  $f_T$  and image encoder  $f_I$ , respectively:

$$\mathbf{H}_T^i = f_T(T_i), \quad \mathbf{H}_I^i = \text{MLP}(f_I(I_i)), \quad (3)$$

where  $\mathbf{H}_T^i \in \mathbb{R}^{d \times n}$  and  $\mathbf{H}_I^i \in \mathbb{R}^{d \times m}$  denote token-level embeddings for the text and image modalities. An MLP projects the image features into the same  $d$ -dimensional space as the text. For each sample pair with an associated relation description  $e_{ij}$ , we extract a global semantic embedding  $\mathbf{h}_E^{ij} = f_T^{\text{EOT}}(e_{ij}) \in \mathbb{R}^d$  from the EOT token.

While contrastive learning encourages positive pairs to be close in the embedding space, different relations imply different notions of similarity. To capture such contextual variations, we compute relation-conditioned features  $\mathbf{z}_x^i(e_{ij})$  for each modality  $x \in \{T, I\}$  using an attention-based aggrega-

tion mechanism (Vaswani et al. 2017).

$$\mathbf{z}_x^i(e_{ij}) = \text{Norm}(\mathbf{A}_x^i(e_{ij})(\mathbf{W}_V \mathbf{H}_x^i)^\top \mathbf{W}_o), \quad (4)$$

where  $\mathbf{H}_x^i$  is the token-level representation,  $\mathbf{W}_V, \mathbf{W}_o \in \mathbb{R}^{d \times d}$  are learnable projections, and  $\text{Norm}(\cdot)$  denotes L2 normalization. The attention weight  $\mathbf{A}_x^i(e_{ij}) \in \mathbb{R}^{1 \times n/m}$  is defined as:

$$\mathbf{A}_x^i(e_{ij}) = \text{softmax} \left( (1 - \beta) \cdot \mathbf{q}_E^{ij} + \beta \cdot \mathbf{B}_x^{ij} \right), \quad (5)$$

$$\mathbf{q}_E^{ij} = (\mathbf{W}_Q \mathbf{h}_E^{ij})^\top (\mathbf{W}_K \mathbf{H}_x^i) / \sqrt{d}, \quad (6)$$

where  $\mathbf{W}_Q, \mathbf{W}_K \in \mathbb{R}^{d \times d}$  are projection matrices and  $\mathbf{h}_E^{ij}$  is the embedding of the relation description  $e_{ij}$ . The first term provides relation-aware contextual attention by allowing the semantic relation  $e_{ij}$  to attend to relevant regions in the modality. The second term  $\mathbf{B}_x^{ij}$  is a binary vector that activates only for intra-sample pairs ( $i = j$ ), highlighting special tokens (e.g., [EOT] or [CLS]) to preserve global consistency. It is designed to capture the inherent alignment between modalities of the same sample, which goes beyond contextual similarity. The coefficient  $\beta \in [0, 1]$  balances the influence of contextual relation guidance and undirected alignment.

**Remark.** CLIP is a special case of our framework with no relation guidance and only cross-modal self-pair training.

Our framework reduces to the original CLIP formulation under two conditions: (1) The attention reduces to global pooling. When  $\beta = 1$  in Equation (5), the relation-conditioned attention degenerates to  $\mathbf{A}_x^i = \text{softmax}(\mathbf{B}_x^{ij})$ , where  $\mathbf{B}_x^{ij}$  is a one-hot vector selecting the summary token. This eliminates the influence of  $e_{ij}$ , and  $\mathbf{z}_x^i(e_{ij})$  becomes functionally equivalent to CLIPs global embedding, which pools modality information without contextual semantics.

(2) The objective reduces to pairwise cross-modal contrast. Since  $\mathbf{B}_x^{ij}$  is only defined for intra-sample pairs ( $i = j$ ), setting  $\beta = 1$  also restricts training to self-pairs. If the contrastive objective is further applied only to cross-modal directions ( $x \neq y$ ), the overall loss reduces to:

$$\mathcal{L} = (\mathcal{L}_{\text{txt-img}} + \mathcal{L}_{\text{img-txt}}) / 2, \quad (7)$$

where each loss term is computed over same-item pairs:

$$\mathcal{L}_{x-y} = - \sum_{(i,i) \in \mathcal{P}} \log \frac{\exp(\text{sim}(\mathbf{z}_x^i, \mathbf{z}_y^i) / \tau)}{\sum_{k \in \mathcal{N}(i)} \exp(\text{sim}(\mathbf{z}_x^i, \mathbf{z}_y^k) / \tau)}. \quad (8)$$

Together with standard in-batch negative sampling, this configuration recovers the CLIP formulation as a special case of RCML.  $\square$

## 4 Experiments

In this section, we first introduce the experimental setup and baseline models. We then evaluate our framework on three multimodal relation-aware tasks. Finally, we provide detailed analyses of the models performance and behavior.

### 4.1 Experimental Setup

We conduct experiments on seven domains of the Amazon Product dataset (Hou et al. 2024): Electronics, Automotive, Office Products, Baby, Pet Supplies, Musical Instruments, and Sports. Each product is associated with a title and an image. Pairs of products are considered related if they are co-purchased by users with shared interests, and each relation is annotated with a natural-language description indicating its semantic context. For each domain, we split the data into training and testing sets with no overlap in product pairs. Further details of the experimental settings and computing environment are provided in the appendix.

### 4.2 Baseline Models

To provide a comprehensive evaluation, we compare our method against several strong visionlanguage baselines. CLIP (Radford et al. 2021) learns aligned imagetext embeddings through large-scale contrastive pretraining. DeCLIP (Li et al. 2021) enhances CLIP by introducing data augmentation and auxiliary objectives to improve robustness. UniCL (Yang et al. 2022) incorporates label supervision to unify representations across modalities and domains. SigLIP (Touvron et al. 2023) replaces CLIPs loss with a sigmoid-based formulation to improve data efficiency, and is trained on a larger dataset. ImageBind (Girdhar et al. 2023) extends contrastive pretraining to multiple modalities including audio and depth; for fair comparison, we focus on its visiontext component. Notably, it uses a much larger model backbone with significantly more parameters than ours.

### 4.3 Downstream Tasks

We evaluate our framework on three tasks designed to test relation-aware multimodal learning under both zero-shot and supervised settings. The first two tasks assess generalization ability without downstream tuning, evaluating whether the model can directly capture semantic alignment guided by relational context. The third introduces a

lightweight MLP to examine whether the learned representations are sufficiently discriminative to support supervised relation reasoning.

**Relation-Guided Retrieval** This task simulates a recommendation-style scenario (Wen et al. 2022; He et al. 2017). Given a source product  $A$  and a semantic relation type (e.g., bought together by people who like fishing), the goal is to retrieve the most relevant target product  $B$  from a candidate set. Each query includes one positive and 20 randomly sampled negatives, forming a 21-way retrieval problem. We report Hit@5 as the primary metric, reflecting realistic recommendation settings where users examine only top-ranked results.

To compute relevance scores, we extract text and image embeddings using RCML and all baselines. We compute five types of similarity: (1) text-text (TT), cosine similarity between the textual embeddings of  $A$  and  $B$ ; (2) image-image (II), cosine similarity between their image embeddings; (3) text-image (TI), from  $A$ s text to  $B$ s image; (4) image-text (IT), from  $A$ s image to  $B$ s text; and (5) average (AVG), cosine similarity between the averaged text and image embeddings of each product. These scores are used to rank candidates and assess how well each model aligns multimodal features under relational context.

As shown in Table 1, our proposed RCML consistently outperforms all baselines across most settings, achieving the best results on 32 out of 35 metrics. This highlights its strong ability to leverage both multimodal content and relational semantics for context-aware feature extraction, leading to superior retrieval performance. Compared to the standard CLIP backbone, RCML improves overall Hit@5 by approximately 30.79%. While DeCLIP and UniCL are also trained with contrastive objectives, they perform poorly on our relation-targeted retrieval task. DeCLIP emphasizes local consistency, and UniCL relies on label-level supervision neither captures contextual alignment across semantically related samples. SigLIP performs relatively well, as its sigmoid-based objective enables more flexible pairwise alignment. However, it lacks explicit relational semantics and falls short in relation-aware scenarios. ImageBind benefits from a powerful image encoder and significantly larger model size, which explains its occasional advantage on image-dominant metrics. Still, without relation conditioning, it underperforms RCML overall.

**Relation Type Prediction** In this task, the model is given a product pair  $(A, B)$  and must identify the most likely semantic relation connecting them from a set of 10 predefined types. For each candidate relation, we compute the similarity between  $A$  and  $B$  under the corresponding relation-conditioned embedding, and select the one with the highest score. Since baseline models do not support relation-specific encoding, we report results only for RCML, using five similarity variants across unimodal and cross-modal configurations. We report Top-3 Accuracy on four datasets where relation types are sufficiently meaningful to support evaluation.

As shown in Figure 2, RCML demonstrates strong performance across all domains, consistently exceeding the 30% random baseline by a substantial margin. Among the five

Similarity	Elec	Auto	Office	Baby	Pet	Music	Sports
CLIP (TT)	37.53	36.04	39.46	35.82	42.19	41.95	43.33
CLIP (II)	31.78	27.33	34.27	29.56	34.66	34.56	35.19
CLIP (TI)	33.44	30.40	36.48	30.63	36.93	39.00	39.45
CLIP (IT)	33.81	32.14	37.92	31.62	37.95	37.51	38.82
CLIP (AVG)	37.08	34.01	39.14	34.66	41.34	42.59	42.87
DeCLIP (TT)	28.46	27.76	30.11	29.06	29.57	28.01	29.13
DeCLIP (II)	24.43	24.83	26.05	26.54	24.74	27.48	25.72
DeCLIP (TI)	23.99	22.46	23.84	23.98	22.95	24.37	24.44
DeCLIP (IT)	25.00	22.38	24.02	24.03	23.55	25.22	23.83
DeCLIP (AVG)	27.50	27.42	29.64	30.66	28.81	29.14	29.20
UniCL (TT)	25.04	25.70	25.37	24.51	25.30	26.80	25.28
UniCL (II)	31.09	29.05	35.78	30.26	35.39	34.83	34.89
UniCL (TI)	24.87	25.14	23.48	22.58	23.56	24.25	23.30
UniCL (IT)	23.74	23.96	23.02	22.47	23.56	23.24	24.37
UniCL (AVG)	29.92	29.18	34.03	29.04	34.58	35.59	33.02
SigLIP (TT)	38.91	36.63	40.79	39.91	41.19	42.41	45.78
SigLIP (II)	36.60	30.57	37.25	33.79	37.66	38.90	41.97
SigLIP (TI)	36.51	33.63	38.00	34.92	40.65	42.29	46.14
SigLIP (IT)	36.09	33.47	38.41	34.40	38.64	41.36	45.42
SigLIP (AVG)	39.69	35.15	40.71	39.17	40.76	43.14	46.62
ImageBind (TT)	40.25	36.73	41.96	41.53	43.73	45.94	48.09
ImageBind (II)	38.93	31.38	39.57	<b>36.43</b>	39.56	<b>41.95</b>	42.47
ImageBind (TI)	38.01	35.22	39.20	35.60	41.46	<b>44.61</b>	46.79
ImageBind (IT)	38.01	34.51	38.90	35.30	40.36	41.66	45.90
ImageBind (AVG)	41.63	35.68	42.94	40.13	43.77	47.07	48.48
RCML (TT)	<b>49.32</b>	<b>44.38</b>	<b>49.22</b>	<b>44.62</b>	<b>54.17</b>	<b>51.29</b>	<b>64.49</b>
RCML (II)	<b>40.09</b>	<b>35.96</b>	<b>42.98</b>	35.10	<b>44.89</b>	40.52	<b>46.77</b>
RCML (TI)	<b>42.49</b>	<b>37.28</b>	<b>43.93</b>	<b>38.42</b>	<b>48.11</b>	41.32	<b>52.66</b>
RCML (IT)	<b>48.00</b>	<b>39.77</b>	<b>46.33</b>	<b>41.20</b>	<b>50.00</b>	<b>43.50</b>	<b>63.36</b>
RCML (AVG)	<b>49.09</b>	<b>44.31</b>	<b>49.64</b>	<b>44.65</b>	<b>55.08</b>	<b>51.53</b>	<b>64.81</b>

Table 1: Hit@5 (%) for Relation-Guided Retrieval on 7 datasets using five similarity measures. **Bold** numbers indicate the best performance in each dataset.

similarity variants, the averaged configuration (AVG) performs best overall reaching 70.4% on *Baby* and 88.9% on *Sports* highlighting the advantage of combining textual and visual cues for relation inference.

**Relation Validity Prediction** Unlike the previous task, which evaluates zero-shot selection among candidate relation types, this task focuses on supervised validation of specific relation instances. Given a product pair ( $A, B$ ) and a candidate relation type, the model must predict whether a relation of that type exists between them. This is formulated as a binary classification problem, and we report classification accuracy as the evaluation metric. For fair comparison, all baseline models are kept frozen, and a lightweight linear classifier is trained on top of their extracted features. The input to the classifier is the concatenation of text and image embeddings from both products, along with the embedding of the relation label. This setup evaluates whether the learned multimodal representations can support relation-aware prediction when supervision is available.

As shown in Figure 3, RCML consistently outperforms all baselines across most datasets. This demonstrates its strong ability to integrate semantic relations into multimodal representation learning. Baselines such as CLIP exhibit significant performance variance for example, achieving 89.44% accuracy on *Office* but only 61.82% on *Baby* indicating

limited generalization across domains. RCML, by conditioning feature extraction on relation semantics, maintains stable and high performance across all settings. SigLIP and ImageBind perform competitively due to their soft supervision and larger model capacity. However, they lack explicit relation-aware mechanisms. As a result, their performance still falls short on tasks requiring fine-grained relational reasoning.

#### 4.4 Further Evaluation and Analysis

We conduct a series of analyses to better understand the effectiveness of our relation-aware framework. These include ablation studies, sensitivity analysis, visualizations, qualitative case studies and model complexity evaluation.

**Ablation Studies.** To evaluate the contributions of different components in our framework, we conduct ablation experiments on the Relation-Guided Retrieval task. Results are averaged over the seven datasets and reported across five similarity types, as shown in Figure 4. We compare five settings: (1) **w/o inter edge**: removes all inter-sample relations, resulting in the largest performance drop (38.68%), which confirms the importance of many-to-many learning across samples. (2) **w/o intra loss**: disables the intra-modal contrastive objective while retaining cross-modal training. The performance drop (8.50%) suggests that intra-modal alignment contributes meaningfully, though it is not the domi-

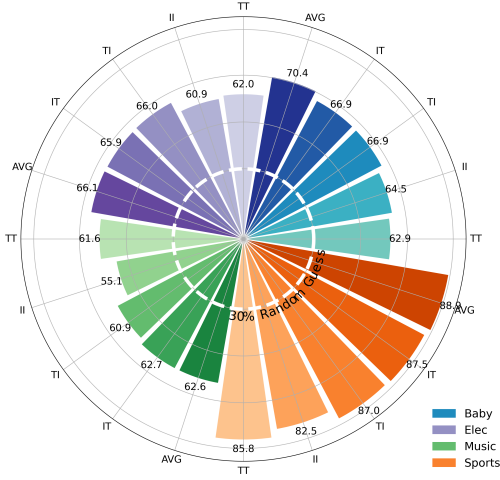


Figure 2: Top-3 accuracy for Relation Type Prediction across five similarity types.

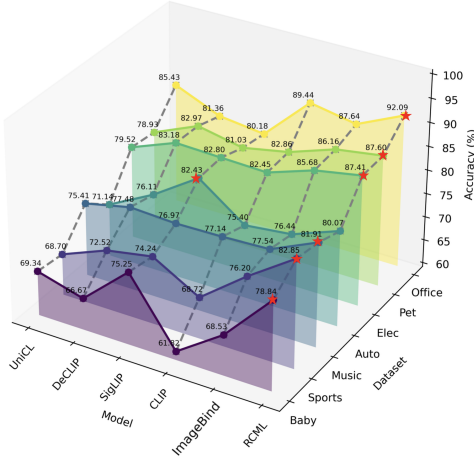


Figure 3: Accuracy (%) on Relation Validity Prediction. ★ denotes the best performance on each dataset.

nant factor. (3) **w/o edge description**: removes the semantic content of relations but retains relation connectivity. The decline (11.60%) highlights the value of contextual guidance in learning relation-aware representations. (4) **Frozen CLIP**: freezes the CLIP encoders and trains only the attention module. The significant drop (37.93%) shows the necessity of end-to-end adaptation for relation-aware learning. (5) **RCML**: our full model achieves the best performance, demonstrating the effectiveness of leveraging semantic relations through many-to-many contrastive supervision. These trends hold consistently across all similarity types, indicating that each component of our framework contributes positively to both unimodal and cross-modal alignment under relational context.

**Sensitivity Analysis.** As defined in Equation (5), the coefficient  $\beta \in [0, 1]$  controls the trade-off between relation-specific contextual attention and undirected alignment via

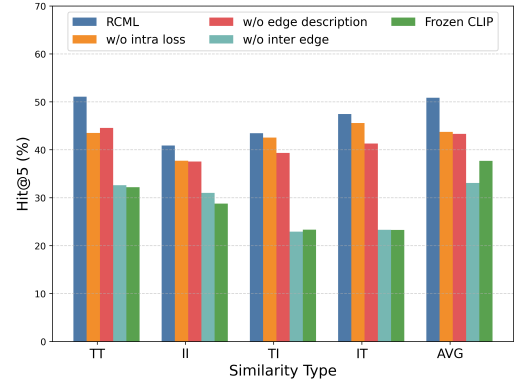


Figure 4: Ablation results across similarity types on Relation-Guided Retrieval.

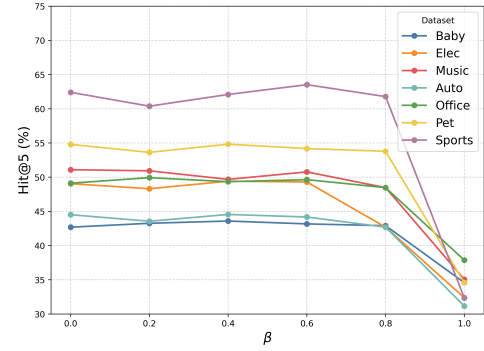


Figure 5: Sensitivity analysis of the attention coefficient  $\beta$  on Relation-Guided Retrieval.

global summary tokens. We evaluate the impact of this balancing coefficient in Figure 5. Model performance remains relatively stable across a broad range of  $\beta$  values (from 0.0 to 0.6), with the best results typically observed around  $\beta = 0.4$  or  $0.6$ . Notably, performance at  $\beta = 0$  using only relation-guided attention is nearly as strong, suggesting that contextual semantics alone provide valuable guidance. However, performance declines gradually at  $\beta = 0.8$  and drops sharply at  $\beta = 1.0$ , where only global tokens from the CLIP encoder are used without any relation-specific modulation. This highlights the importance of integrating both global and contextual signals for relational alignment.

**Visualization.** To qualitatively evaluate our framework, we visualize the feature spaces learned by RCML and CLIP using t-SNE. We randomly sample a subset of products and extract their embeddings under the relation “Users who like to purchase Sports & Outdoor Recreation Accessories tend to buy together.” As shown in Figure 6, RCML produces more compact and semantically meaningful clusters. For example, items such as bike bells, chainstay protectors, and wet chain lubes are grouped closely together, reflecting their shared relevance to cycling enthusiasts. In contrast, CLIP embeddings appear more dispersed, indicating a lack of relation-aware organization. These results demon-



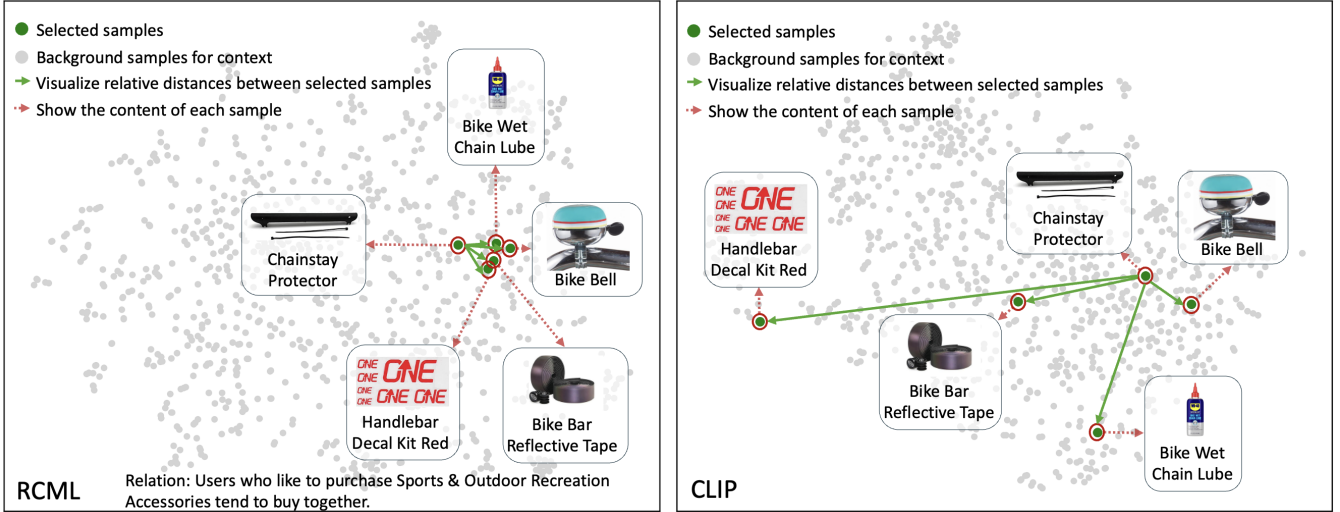


Figure 6: t-SNE visualization of multimodal embeddings under the semantic relation *Users who like to purchase Sports & Outdoor Recreation Accessories tend to buy together*. RCML (left) forms more coherent clusters than CLIP (right), suggesting superior organization of relation-aware representations.

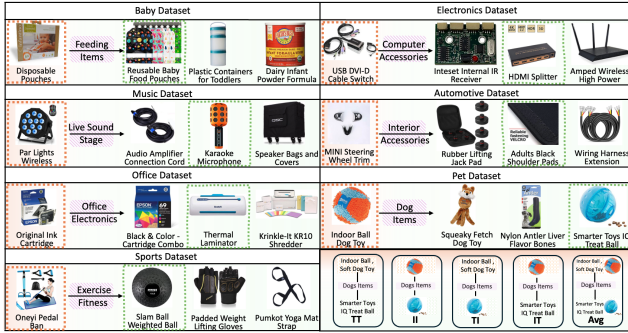


Figure 7: Case study showing the top-3 predictions (out of 21 candidates) ranked by our model in Relation-Guided Retrieval. Highlighted items correspond to the query, relation context, and correct targets.

strate that our model goes beyond surface-level similarity, capturing functional and intent-driven associations.

**Case Study.** Figure 7 shows representative examples from the Relation-Guided Retrieval task, one per dataset. In each case, the leftmost item (highlighted with a yellow dashed box) is the query  $A$ , and the top-3 retrieved candidates appear on the right. The semantic relation used for retrieval is displayed on the connecting arrow. Ground-truth targets are marked with green boxes. As shown, our model consistently retrieves contextually relevant items aligned with the intended relation. For instance, given a karaoke microphone and the relation *Live Sound & Stage*, the model retrieves accessories such as speaker bags and audio connectors, rather than irrelevant items with visual or textual similarity. The bottom panel illustrates the five similarity configurations (TT, II, TI, IT, AVG) used in scoring, which provide complementary perspectives for retrieval.

**Efficiency and Model Size.** Table 2 compares inference latency and model size across all methods. Despite incorporating relation-aware components, RCML remains efficient (14.32 ms/sample, 152.33M parameters), only slightly above CLIP and DeCLIP. Notably, ImageBind incurs much higher cost (35.90 ms/sample, 1200M+ parameters) while still underperforming RCML on most tasks, making it less practical for retrieval scenarios. These results show that relation conditioning introduces minimal overhead while delivering superior performance.

## 5 Conclusion

We presented RCML, a contrastive learning framework that conditions multimodal representation learning on semantic relations. Across multiple datasets and tasks, RCML consistently outperforms strong baselines. Further analysis shows that RCML delivers robust performance across domains and effectively organizes items under relation-defined contexts by bringing semantically related products closer in the embedding space. Beyond its empirical strength, RCML offers a general and adaptable learning paradigm that can be integrated into more advanced multimodal systems to support relation-aware representation learning.

Model	Inference Time (ms/sample)	#Params (M)
CLIP	9.17	151.28
DeCLIP	11.29	158.76
UniCL	21.93	150.70
SigLIP	9.89	203.16
ImageBind	35.90	1200.78
RCML	14.32	152.33

Table 2: Inference time and parameter count for each model.

## Appendix: Experimental Details

**Implementation Framework.** Our model is implemented using the Hugging Face `CLIPModel` and `CLIPProcessor`, which wrap the OpenAI CLIP architecture. We use the ViT-B/32 backbone for all experiments.

**Training Configuration.** We conduct grid search over multiple hyperparameters and select the best setting based on validation performance. The final configuration is:

- **Batch size:** 512
- **Optimizer:** AdamW
- **Learning rate:**  $5 \times 10^{-5}$ , with cosine decay
- **Epochs:** Early stopping applied based on validation performance; training typically converged within 3 epochs
- **Contrastive temperature  $\tau$ :** 0.1
- **Intra-modal weight  $\lambda$ :** 0.5
- **Attention balance coefficient  $\beta$ :** 0.6

**Computing Environment.** All experiments are conducted on a single NVIDIA RTX A6000 GPU with 48GB memory. Software versions are:

- Python 3.9
- PyTorch 1.12
- Transformers 4.26
- CUDA 11.6

**Reproducibility.** We fix the random seed at 42 for all experiments. All preprocessing scripts, training code, and evaluation metrics will be released upon publication to facilitate reproducibility.



## References

- Alayrac, J.-B.; Donahue, J.; Luc, P.; Miech, A.; Cabi, S.; Radford, A.; Misra, I.; Clark, A.; Hsiao, J.; Huang, C.; et al. 2022. Flamingo: a Visual Language Model for Few-Shot Learning. *arXiv preprint arXiv:2204.14198*.
- Arora, S.; Liang, Y.; and Ma, T. 2019. A theoretical analysis of contrastive unsupervised representation learning. In *Proceedings of ICML*, 5628–5637.
- Chen, Y.; Zhu, Q.; Ma, Y.; Zhang, J.; Zhang, Z.; and Xiong, D. 2020. Graphflow: Exploiting conversation flow with graph neural networks for conversational machine comprehension. In *Proceedings of the 28th International Conference on Computational Linguistics*, 2482–2494.
- Gadre, S.; Li, X.; Li, Y.; Zhao, Z.; Lin, K.; Zhang, H.; Kirillov, A.; Joulin, A.; Zhai, X.; Dai, Z.; et al. 2023. DataComp: In search of the next generation of multimodal datasets. In *Proceedings of the IEEE/CVF Conference on Computer Vision and Pattern Recognition*, 26452–26465.
- Girdhar, R.; Han, W. L.; Joulin, A.; Synnaeve, G.; Mairal, J.; and Misra, I. 2023. ImageBind: One embedding space to bind them all. *arXiv preprint arXiv:2305.05665*.
- He, X.; Liao, L.; Zhang, H.; Nie, L.; Hu, X.; and Chua, T.-S. 2017. Neural collaborative filtering. In *Proceedings of WWW*.
- Hou, Y.; Li, J.; He, Z.; Yan, A.; Chen, X.; and McAuley, J. 2024. Bridging Language and Items for Retrieval and Recommendation. *arXiv preprint arXiv:2403.03952*.
- Jia, C.; Yang, Y.; Xia, Y.; Chen, Y.-T.; Parekh, Z.; Pham, H.; Le, Q. V.; Sung, Y.-H.; Li, Z.; and Duerig, T. 2021. Scaling up visual and vision-language representation learning with noisy text supervision. In *International Conference on Machine Learning*, 4904–4916. PMLR.
- Jiang, H.; Misra, I.; Rohrbach, M.; Wang, X.; Learned-Miller, E.; and Fei-Fei, L. 2020. Cmg: Cross-modal graph modeling for visual question answering. In *European Conference on Computer Vision*, 206–223. Springer.
- Kipf, T. N.; and Welling, M. 2017. Semi-supervised classification with graph convolutional networks. In *Proceedings of the International Conference on Learning Representations (ICLR)*.
- Li, J.; Zhang, D.; Natarajan, V.; Gao, J.; Baldridge, J.; and Lazebnik, S. 2023. BLIP-2: Bootstrapping Language-Image Pre-training with Frozen Image Encoders and Large Language Models. In *International Conference on Learning Representations (ICLR)*.
- Li, L. H.; Yatskar, M.; Yin, D.; Hsieh, C.-J.; and Chang, K.-W. 2021. Supervision exists everywhere: A data efficient contrastive language-image pretraining paradigm. In *International Conference on Learning Representations*.
- Liu, F.; Mao, J.; Wang, Y.; Zheng, Q.; Wu, Y.; and Yuille, A. L. 2020. Graph structured network for image-text matching. In *Proceedings of the IEEE/CVF Conference on Computer Vision and Pattern Recognition*, 10921–10930.
- Mu, J.; Kirillov, A.; Zhai, X.; Misra, I.; Wightman, R.; Collobert, R.; Joulin, A.; Touvron, H.; Mahadevan, S.; Yalniz, I. Z.; et al. 2021. SLIP: Self-supervision meets language-image pre-training. In *European Conference on Computer Vision*.
- Names, A. 2024. LLM2CLIP: Powerful Language Model Unlock Richer Visual Representations. *arXiv preprint arXiv:2411.04997*.
- Qiao, Y.; Zhang, W.; Xu, J.; Ren, X.; and Sun, X. 2023. Mutual-Enhanced Incongruity Learning Network for Multi-Modal Sarcasm Detection. In *Proceedings of the AAAI Conference on Artificial Intelligence*, volume 37, 10344–10352.
- Radford, A.; Kim, J. W.; Hallacy, C.; Ramesh, A.; Goh, G.; Agarwal, S.; Sastry, G.; Askell, A.; Mishkin, P.; Clark, J.; et al. 2021. Learning transferable visual models from natural language supervision. In *International conference on machine learning*, 8748–8763. PMLR.
- Schuhmann, C.; Beaumont, R.; Vencu, R.; Gordon, C.; Wightman, R.; Cherti, M.; Coombes, T.; Katta, A.; Mullis, C.; Schreiber, A.; et al. 2022. LAION-5B: An open large-scale dataset for training next generation image-text models. *arXiv preprint arXiv:2210.08402*.
- Touvron, H.; Misra, I.; Douze, M.; Synnaeve, G.; Massa, F.; Jegou, H.; and Bojanowski, P. 2023. Scaling and evaluating zero-shot models. *arXiv preprint arXiv:2302.10866*.
- Vaswani, A.; Shazeer, N.; Parmar, N.; Uszkoreit, J.; Jones, L.; Gomez, A. N.; Kaiser, .; and Polosukhin, I. 2017. Attention Is All You Need. In *Advances in Neural Information Processing Systems (NeurIPS)*, volume 30.
- Veličković, P.; Cucurull, G.; Casanova, A.; Romero, A.; Lio, P.; and Bengio, Y. 2018. Graph attention networks. In *Proceedings of ICLR*.
- Wang, H.; Shi, C.; Wang, Y.; Liu, Z.; and Song, G. 2022a. CMKG: Cross-modal knowledge graph reasoning for explainable recommendation. In *Proceedings of the 28th ACM SIGKDD Conference on Knowledge Discovery and Data Mining*, 1710–1720.
- Wang, Z.; Yang, J.; Zhang, X.; Zhang, Y.; Wang, Q.; Yang, L.; Yuan, L.; and Zhang, L. 2022b. Git: A generative image-to-text transformer for vision and language. In *Proceedings of the IEEE/CVF Conference on Computer Vision and Pattern Recognition*, 17177–17187.
- Wen, H.; Qi, S.; Zhang, Y.; and Yu, W. 2022. CAT: Contrastive Attributed Network Embedding. In *Proceedings of the Web Conference 2022 (WWW)*.
- Yang, F.; Ma, X.; Wu, Y.; Zhang, Q.; Dong, Y.; Cheng, J.; and Liu, W. 2022. Unified contrastive learning in image-text-label space. In *Proceedings of the IEEE/CVF Conference on Computer Vision and Pattern Recognition*, 19163–19173.
- Yao, Y.; Sun, Y.; Wang, N.; Yu, D.; Chen, Y.; and Wang, S. 2019. Graph-based reasoning over heterogeneous external knowledge for commonsense question answering. In *Proceedings of the AAAI Conference on Artificial Intelligence*, volume 33, 8879–8886.
- Zhai, X.; Kolesnikov, A.; Mustafa, B.; Beyer, L.; Steiner, A.; Khosla, P.; Biderman, S.; Riquelme, C.; Houlsby, N.; Barham, P.; et al. 2022. LiT: Zero-Shot Transfer

with Locked-image Text Tuning. In *Proceedings of the IEEE/CVF Conference on Computer Vision and Pattern Recognition (CVPR)*, 18123–18133.

Zhang, X.; Li, H.; He, X.; Ma, J.; and Zhou, Z. 2023. M2GCN: Multi-modal Graph Convolution Network for Personalized Micro-video Recommendation. In *Proceedings of the 46th International ACM SIGIR Conference on Research and Development in Information Retrieval*, 2308–2317.